Design and Performance Model of Probe-Fed Rectangular Patch Antenna for LTE 2300 MHz Smart Phone and Portable Computer Applications

Settapong Malisuwan, Wassana Kaewphanuekrungsi, Jesada Sivaraks, and Nattakit Suriyakrai

***Abstract*—In this research, a simple model to design and demonstrate the performance of a probe-fed rectangular patch antenna isproposed. The proposed model is divided into two parts which are the theoretical formulations of the patch antenna integrated with the frequency-dependent Smith-chart method and the Cole-Cole representation to demonstrate the performance of the microstrip antenna. The antenna designed in this research will be used for LTE 2300 MHz smart phone and portable computer applications. It is pertinent for applications in the range of 2300-2360 MHz with the resonant frequency at 2.33 GHz. The proposed model can be used to design a single and multilayer microstrip patch antenna and this is valuable contribution on literature of computer-aided microwave circuit designs.**

***Index Terms*—Performance, frequency-dependent, patch antenna, LTE, 2300 MHz.**

I. Introduction

Microstrip structure is one of the most popular types of planar transmission lines, primarily because it can easily integrate with other passive and active microwave devices. The relevant design equations in closed-form using semi-empirical strategies specifying the frequency-dependent, effective dielectric permittivity concept and dispersion characteristics of a microstrip structure have been derived in the existing literature as elaborated in [1] [2]. Most computer-aided design (CAD) systems used these algorithms with built-inmicrostrip design capabilities but simple calculation methods for microstrip structure parameters by hand-calculator and/or by personal computer are required for preliminary design and for quick circuit evaluation purposes. It is necessary to consider observe physical considerations of microstrip circuits on a step-by-step basis. So, researcherswant simple methods, which are same time sufficient to explain the physical aspects of microstrip circuits more accurately.

Rectangular patch antennas have attracted tremendous attention from researchers [3]-[12]. However, radome or superstrate rectangular patch antennas are not widely discussed in academic literature [3]-[12]. Superstrate is significant as it is used as prevention from environmental hazard and enhances the antenna's performance [13]. The patch with substrate-superstrate combined geometry function swell under a noisy environment. Superstrate decreases the bandwidth of the antenna therefore it is pertinent for filter design [14].

The main contribution of this paper is to design a probe-fed rectangular patch antenna for LTE 2300 MHz and propose the model of the microstrip antenna performance based on the Cole-Cole diagram representation [15]. To achieve this goal, an approach that uses the Debye relation [16] is introduced to portray such frequency-dependent characterization of a microstrip structure.

II. LTE in the 2300 MHz Band

In wireless communication spectrum, the 100MHz portion of available spectrum in the 2300-2400MHz band (the 2300MHz band hereafter) may play a key role in helping to meet the EU's Digital Agenda for Europe and RSPP objectives. This represents the largest near-term opportunity for new LTE spectrum across Europe. 2300 MHz is defubed as a 3GPP euTRAN band in Time Division Duplex or TDD. LTE-TDD is becoming significant and gaining popularity worldwide as it is commonly considered in the evolution path of any wireless cellular TDD technology (TD-SCDMA, UTRA-TDD and WiMAX™). LTE-TDD is an integral part of the 3GPP standards, sharing significant common properties with LTE-FDD and offering comparable performance characteristics with similar high-spectral efficiency.

A total of 43 LTE-TDD-2300MHz compatible devices were commercially available in April 2012. Considerable economies of scale will be reached by the end of 2013 as shown in Table I.

TABLE I: Commercial Availability of LTE Devices (source: GSA)

LTE TDD	# of commercial devices
2300 MHz - Band 40	43
2600 MHz - Band 38	45
2600 MHz - Band 41	5
LTE FDD	# of commercial devices
700 MHz	170
800 MHz - Band 20	72
1800 MHz - Band 3	75
2600 MHz - Band 7	94
800 / 1800 / 2600 MHz	57
AWS - Band 4	72

The 2300MHz band is already specified as a 3GPP band for both TD-SCDMA and LTE-TDD since LTE Release 8 as shown in Table II.

Manuscript received June 20, 2013; revised June 28, 2013; accepted July 15, 2013. This work was supported by National Broadcasting and Telecommunications Commission.

The authors are with the National Broadcasting and Telecommunications Commission (e-mail: settapong.m@nbtc.go.th, wassana.k@nbtc.go.th, jesada.s@nbtc.go.th, nattakit.s@nbtc.go.th).

DOI: 10.7763/IJCCE.2013.V2.277

TABLE II: 3GPP E-UTRA FREQUENCY BANDS - TS 36.104 V8.1.0 (2008-03)

E-UTRA Operating Band	Uplink (UL) operating band BS receive, UE transmit	Downlink (DL) operating band BS receive, UE receive	Duplex Mode
	FUL_low - FUL_high	FDL_low - FDL_high	
40	2300 MHz - 2400 MHz	2300 MHz - 2400 MHz	TDD

Intra-band Carrier Aggregation (CA) within the 2300MHz was already specified in 3GPP Rel. 10, while inter-band CA involving the 2300 MHz band has not been specified at this time. ITU-R WRC-07 identified the 2300MHz band as suitable for the IMT family of technologies in all three ITU-R regions while, according to footnote 5.384A22, this allocation does not preclude administrations from permitting deployment of other radio-communication services within this band.

The 2300 MHz range has been allocated to fixed, mobile, radiolocation and amateur services (the first two on a primary basis with the second two on a secondary basis). In many cases, depending on national circumstances, these applications may not use the entire band in all locations or at all times.

III. THEORETICAL FORMULATIONS OF THE RECTANGULAR PATCH ANTENNA

To achieve the simple design model as a major objective of this research, we adopt the model proposed in the literature in [15] and apply the frequency-dependent Smith-Chart (FDSC) model from [16] to reduce errors from very high frequencyeffects. The FDSC model will be discussed later in Section IV.

The radome loaded patch can receive the signal even while there is noise. In designing, theradome loaded patch the resonant frequency is a key parameter because it is used to determine the dimensions of the patch. So, the accurate computation of resonant frequency is very important.

The resonant frequency of radome loaded rectangular patch antenna is illustrated in Fig. 1, iswritten as [17]

$$f_{r,mn} = \frac{c}{2\sqrt{\varepsilon_{r,eff}}}((m/b_e)^2 + (n/a_e)^2)^{1/2} \quad (1)$$

Where, c is the velocity of light in free space, $\varepsilon_{r,eff}$, b_e, a_e are the optimal dielectric constant, length and width respectively of a rectangular patch antenna with and without radome.

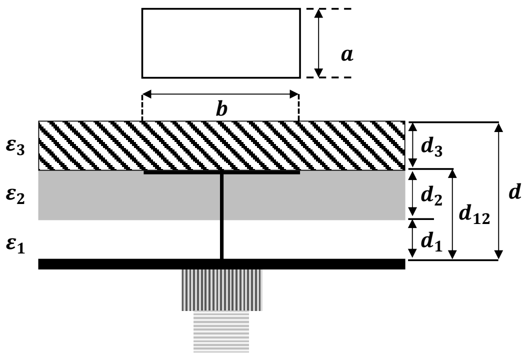

Fig. 1. A randome loaded patch antenna.

The dielectric constant of the antenna effectiveness is improvedbecause of dielectric loading. To compute $\varepsilon_{r,eff}$ of radome loaded rectangular patch antenna, variety of techniques are available [3], [4], [7]-[11]. Among them, conformal mapping techniques [7] [10] [11] is more accurate but involves m mathematical steps. In this paper, we adopt a very simple expression that involves less mathematical steps for computing $\varepsilon_{r,eff}$ as

$$\varepsilon_{r,eff} = F_1 + F_2 \quad (2)$$

The first term (F_1) of this equation represents the effective permittivity of the patch without dielectric loading. Due to dielectric loading the effective permittivity is improved and this improvement is counted by introducing an empirical relation (F_2). F_1andF_2 may be expressed as

$$F_1 = \frac{\varepsilon_{re}+1}{2} + \frac{\varepsilon_{re}-1}{2}(1 + \frac{12d_{12}}{2^{2.585}a})^{-1/2} \quad (3)$$

$$F_2 = 0.00377 \left(\frac{a}{d_{12}}\right)\left(\frac{d_3}{d_2}\right)\left(\frac{\varepsilon_{r3}}{\varepsilon_{r2}}\right) \quad (4)$$

$$\varepsilon_{re} = \frac{\varepsilon_{r1}\varepsilon_{r2}\varepsilon_{r3}d}{\varepsilon_{r2}\varepsilon_{r3}d_1+\varepsilon_{r1}\varepsilon_{r3}d_2+\varepsilon_{r1}\varepsilon_{r2}d_3} \quad (5)$$

The actual length is enhanced due to the fringing field at the end of patch and this is termed as effective length b_e. The effective length b_e of substrate-superstrate combined geometry may be expressed as [18]

$$b_e = b + 2\Delta b \quad (6)$$

where, Δb is the extension of length due to fringing field of substrate-superstrate combined geometry. The fringing fields are very much dependent on the relative characteristics of the substrate and radome as indicated in [19].

Different expressions are available in open literature for computing Δb without radome. Among them, [18] have provided more accurate expression for computing Δb without radome. We have employed this expression for computing Δb with radome as

$$\Delta b = d_{12}(p_1p_2p_3/p_4)(7)$$

$$p_1 = 0.434907(\frac{\varepsilon_{r,eff}^{0.81} + 0.26}{\varepsilon_{r,eff}^{0.81} - 0.189})(\frac{(a_e/d_{12})^{0.8544} + 0.236}{(a_e/d_{12})^{0.8544} + 0.87})$$

$$p_2 = 1 + (\frac{(a_e/d_{12})^{0.371}}{2.358\varepsilon_{r,eff} + 1})$$

$$p_3 = 1 + \frac{0.5274arctan[0.084(a_e/d_{12})]^{1.9413/p_2}}{\varepsilon_{r,eff}^{0.9236}}$$

$$p_4 = 1 + 0.0377\arctan\left[0.067\left(\frac{a_e}{d_{12}}\right)^{1.456}\right]\{6 - 5\exp(0.036(1-\varepsilon_{r,eff}))\}$$

$$p_5 = 1 - 0.218\exp(-7.5a_e/d_{12})$$

The width is also enhanced due to fringing fields and expressed as a_e. We have used the expression of a_e that was given by [20] without randome for computing a_e with radome as

$$a_e = \sqrt{\varepsilon_{re}/\varepsilon_{r,eff}}\left[a + 0.882d_{12} + 0.164\frac{d_{12}(\varepsilon_{re}-1)}{\varepsilon_{re}^2}\right] + \sqrt{\varepsilon_{re}/\varepsilon_{r,eff}}\frac{d_{12}(\varepsilon_{re}+1)}{\pi\varepsilon_{re}}\left[\ln\left(\frac{a}{2d_{12}}\right) + 1.451\right] \quad (8)$$

$$R(\rho) = \frac{4\mu_r\eta_0 Q_T d_{12} b_e}{\pi\lambda_r a_e} cos^2\left[\pi\left(\frac{0.5b-\rho}{b_e}\right)\right] \quad (9)$$

The V.S.W.R. less than 2.0 bandwidth, efficiency and gain are computed from [46] as

$$B.W = \frac{1}{\sqrt{2}}Q_r^{-1} \quad (10)$$

where Q_r is the radiation loss.

IV. The Frequency-Dependent Smith-Chart Model (FDSC)

The FDSC model has been proposed in the literature [21]. The concept of microstrip-based Cole-Cole diagram is applied to construct a frequency-dependent (lossy) Smith-chart to analyze microstrip line characteristics [17], [21], [22]. Before deriving the frequency-dependent Smith-chart relations, the capacitance parameter in microstrip-line system can be considered. The capacitance per unit length of the classical parallel-plate capacitor can be expressed as [23]

$$C = \varepsilon\frac{w}{h} \quad (11)$$

A simple frequency-dependent capacitance of the parallel-plate capacitor can be modeled in terms of any frequency-dependent attributes of ε. That is,

$$C(\omega) = \varepsilon_0\varepsilon^*(\omega)\frac{w}{h} \quad (12)$$

where$\varepsilon^*(\omega)$ is a complex permittivity :

$$\varepsilon^*(\omega) = \varepsilon'(\omega) - j\varepsilon''(\omega) \quad (13)$$

Referring to the equivalent Cole-Cole diagram deduced for a parallel-plate microstrip line in is derived [21] and then we can obtain the frequency-dependent characteristic impedance $(Z_0'(\omega))$given by:

$$Z_0'(\omega) = \sqrt{\frac{L}{C[A(\omega)-jB(\omega)]}} = \frac{Z_0}{\sqrt{A(\omega)-jB(\omega)}} \quad (14)$$

where $A(\omega)$ and $B(\omega)$ can be found in [21].

Now, the frequency-dependent (lossy) Smith-chart can be constructed by applying $Z_0'(\omega)$ into normalized terminal impedance expression after the procedure is done for the Smith-chart. Therefore, the normalized terminal impedance Z_L' is

$$Z_L' = \frac{Z_L}{Z_0'(\omega)} = br + jbx \quad (Dimensionless) \quad (15)$$

where r and x are the normalized resistance and normalized reactance, respectively, and $b = \sqrt{A(\omega) - jb(\omega)}$.

Corresponding, the voltage reflection coefficient of present Smith chart can be expressed as:

$$\Gamma' = \Gamma_r' + j\Gamma_i' = \frac{Z_L'-1}{Z_L'+1} \quad (16)$$

Or

$$Z_L' = \frac{Z_L}{Z_0'(\omega)} = br + jbx = \frac{(1+\Gamma_r')+j\Gamma_i'}{(1-\Gamma_r')-j\Gamma_i'} \quad (17)$$

Now, the desired sets of equations depicting the modified Smith-chart are:

$$\left(\Gamma_r' - \frac{br}{1+br}\right)^2 + \Gamma_i'^2 = \frac{1}{(1+br)^2} \quad (18)$$

And

$$(\Gamma_r' - 1)^2 + \left(\Gamma_i' - \frac{1}{bx}\right)^2 = \left(\frac{1}{bx}\right)^2 \quad (19)$$

It can be observed that when the lossy characteristics (substrate loss, conductor loss, and frequency-dependent characteristic impedance of the microstrip line) are included in the calculation. As well known in lossy transmission linetheory that, when attenuation as a function of line-length is plotted on the Smith chart, it takes the form of a spiral [21].

V. The Cole-Cole Representation: The performance model

A. Theory of Dielectric Behavior

The quantity of dielectric constant and dissipation factor is essential in designing a device especially for microelectronic equipments.

Debye [24] illustrates the relaxation of polarization with a single relaxation time. He showed that non-interacting dipoles are free to rotate in opposition to much resistance in a fluid like medium. The equation for complex permittivity is

$$\varepsilon^* = \varepsilon_\infty + \frac{\varepsilon_0-\varepsilon_\infty}{1+i\omega\tau} \quad (20)$$

where ε_0= Dielectric constant at low frequency
ε_∞= Dielectric constant at high frequency
ω = Angular frequency
τ = Relaxation time

According to Frohlich, the real and imaginary part of the dielectric constant are given by

$$\varepsilon' = \varepsilon_\infty + \frac{\varepsilon_0-\varepsilon_\infty}{1+\omega^2\tau^2} \text{ and } \varepsilon'' = \left(\frac{\varepsilon_0-\varepsilon_\infty}{1+i\omega\tau}\right)\omega\tau \quad (21)$$

The maximum value of ε' and ε'' is,

$$\varepsilon' = \frac{\varepsilon_0+\varepsilon_\infty}{2} \text{ and } \varepsilon'' = \frac{\varepsilon_0-\varepsilon_\infty}{2} \quad (22)$$

$$\varepsilon_0 - \varepsilon_\infty = \left(\frac{3\varepsilon_0}{2\varepsilon_0+\varepsilon_\infty}\right)\left(\frac{\varepsilon_0+2}{3}\right)\frac{4\pi ng\mu^2}{3kT} \quad (23)$$

where n = Dipole Moment

g = Parameter related to dipole interaction
T = Temperature

On eliminating the parameter ωτ between the two equations and rearranging the two parameters (ε' and ε'') we get,

$$[\varepsilon' - \frac{\varepsilon_0+\varepsilon_\infty}{2}]^2 + \varepsilon''^2 = [\frac{\varepsilon_0-\varepsilon_\infty}{2}]^2 \quad (24)$$

The above equation is of a circle of radius $\frac{\varepsilon_0-\varepsilon_\infty}{2}$. Only the semicircle over which ε” is positive has physical significance. Materials with single relaxation time yield a semicircle in ε’ and ε” plane.

B. Microstrip-Based Equivalent Relaxation Process: Cole-Cole Representation

The method for analyzing the performance of a microstrip structure using the concept of Cole-Cole diagram is proposed in [15]. This paper is the extended study on the multilayered microstrip antenna.

The concept of dielectric relaxation can be used to characterize the frequency-dependent microstrip structure performance. For this purpose the real part of the Debye relation can be equated to the equivalent frequency-dependent permittivity deduced for a microstrip. That is,

$$\varepsilon_u'(\omega) = \varepsilon_{eff}(\omega) = \left[\varepsilon_r + \frac{\varepsilon_{eff}(0)-\varepsilon_r}{1+Q(\omega)}\right] \quad (25)$$

From Kirschning and Jansen’ frequency-dependent effective permittivity in Eqn. (25), it can be equated to the real part of ε^* in Eqn. (21) as follows.

$$\varepsilon_r + \frac{\varepsilon_{eff}(0)-\varepsilon_r}{1+Q(\omega)} = \varepsilon_\infty + \frac{\varepsilon_s-\varepsilon_\infty}{1+4\pi^2(\omega/\omega_r)^2} \quad (26)$$

This gives,

$$\varepsilon_r = \varepsilon_\infty = \varepsilon_0 \quad (27)$$

$$\varepsilon_{eff}(0) = \varepsilon_s \quad (28)$$

$$\tau_0 = \frac{\sqrt{Q(\omega)}}{\omega} \quad (29)$$

Now, an “imaginary part” of the equivalent permittivity of a microstrip system can be obtained by applying Eqns. (27) (28) (29) into the imaginary part of ε^* in Eqn. (21). Hence, the imaginary part of Cole-Cole expression for a microstrip system can be written as

$$\varepsilon_u''(\omega) = \left[\frac{(\varepsilon_{eff}(0)-\varepsilon_r)\sqrt{Q(\omega)}}{1+Q(\omega)}\right] \quad (30)$$

Hence, the complex permittivity of microstrip system in compact form can be written as:

$$\varepsilon_u''(\omega) = \varepsilon_r + \frac{\varepsilon_{eff}(0)-\varepsilon_r}{1+j(1/2\pi)(\omega_0/\omega)} \quad (31)$$

In theory, the maximum points of semi-circles in the Cole-Cole patterns correspond to maximum Debye loss in a dielectric material [25] but, in respect to themicrostrip system, these points can be used to depict the maximum reactive (capacitive) energy confined within the microstrip structure. That is pertinent to the maximum value point (A) in Fig. 2(a). Therefore, it can be considered that the microstrip geometry holds the field within itself, rather than letting it fringe out.

That is, pertinent to these maximum value points (A) in Fig. 2(a), it can be considered that the microstrip geometry holds the field within itself, rather than letting it fringe out.

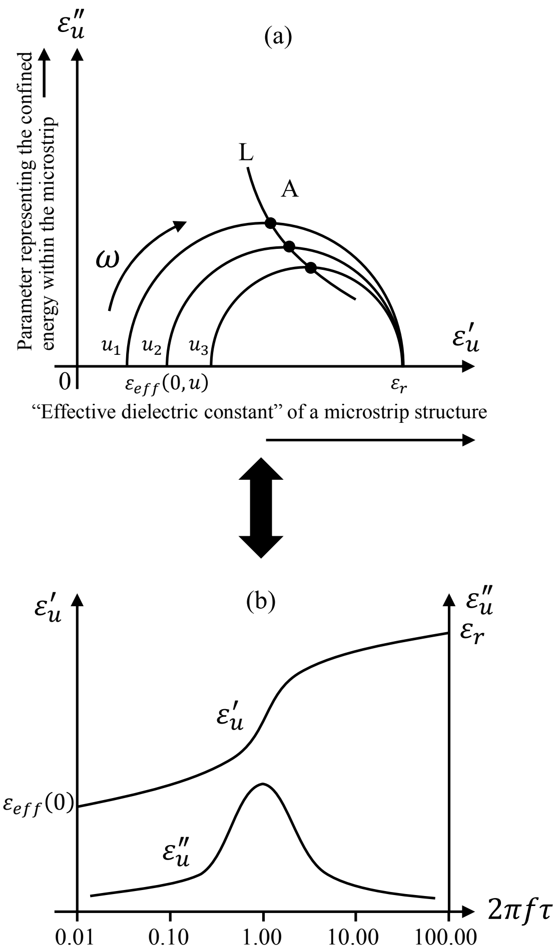

Fig. 2. (a) Cole-Cole representation of reactive relaxation of a microstrip structure with $u = (w/\lambda)(h/\lambda)$ and $u_1<u_2<u_3$
(b) Equivalent Debye relation: microstrip-based.

VI. The Design Procedure of the Proposed Model for LTE 2300 MHz

The proposed procedure in this research is shown in Fig. 3. In the first step, all required characteristics of the antenna need to be identified. We start with the resonant frequency and bandwidth because they are the primary parameters to determine the dimension of the patch. For the second step , we use initial values from the first step to calculate all essential parameters such as ε_{r1}, ε_{r2}, ε_{r3}, a, b, d_1, d_2, d_3, and d to adjust the resonant frequency as close as possible to 2.33 GHz by integrating with FDSC method to reduce errors due to effects of very high frequency in GHz range. The reason that we choose the frequency at 2.33 GHz as the resonant frequency is to operate the proposed antenna in the range of 2.30 - 2.36 GHz (60 MHz bandwidth). In the final step, we use the final results to illustrate the performance of the patch antenna.

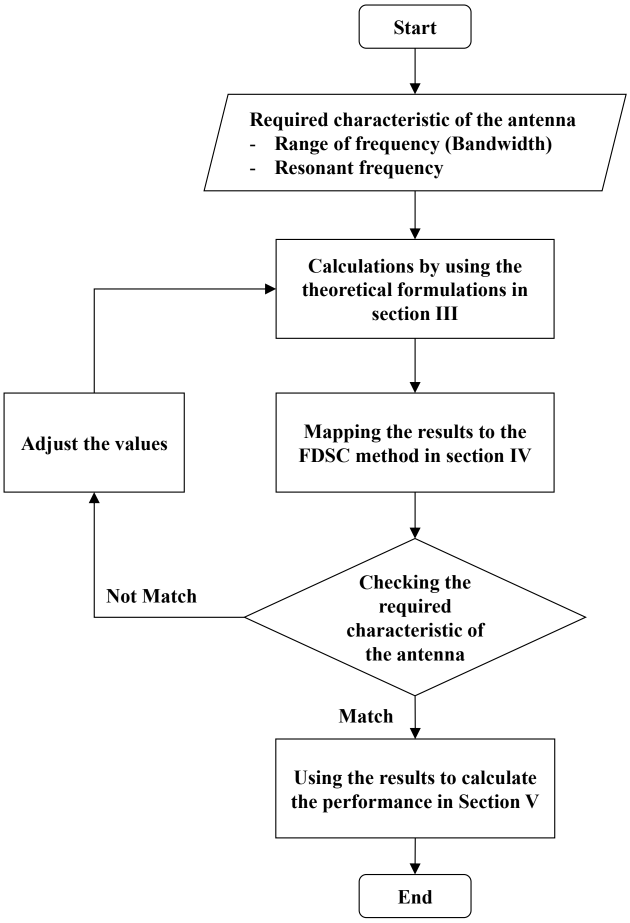

Fig. 3. The procedure of the proposed model.

VII. Simulations and Results

A. Antenna Design Results

Based on the required frequency range of LTE 2300 MHz, 2300 – 2360 MHz, as the tentativerefarming spectrum planning in Thailand, we used the resonant frequency at 2.33 GHz and 60 MHz for bandwidth. We found out in the literature [*] that the initial values of the rectangular patch antenna at 2.347 GHz have to start the procedure in Section V with $\varepsilon_{r1} = 1.0$, $\varepsilon_{r2} = 2.33$, $\varepsilon_{r3} = 1.0$, $d1$=0.0 mm., $d3$=0.0 mm. However, when we ran through the next step by applying the FDSC method with the initial values, we finally received the required antenna structure as shown in Table III to maintain the required resonant frequency at 2.33 GHz with 60 MHz bandwidth.

TABLE III: The Required Antenna Structure

a (mm)	57.5
b (mm)	38.5
ε_{r1}	1.0
ε_{r2}	2.33
ε_{r3}	1.0
d_1 (mm)	0.0
d_2 (mm)	3.175
d_3 (mm)	0.0

C. Performance of the Proposed Antenna

Considering the performance of the proposed antenna in Table III, the simulation results in Fig. 4 indicate that the nonfringing part of the reactive energy in the antenna increases when the b/d_2 ratio reduces.

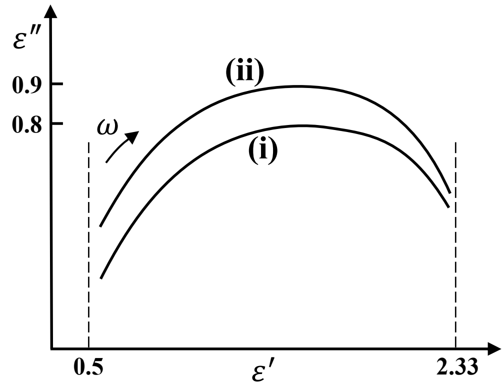

Fig. 4. Cole-Cole diagram of the proposed antenna (i) $b/d_2 = 38.5/3.175 = 12.26$ (ii) $b/d_2 = 10$ when $a = 57.5\text{mm}\varepsilon_{r1} = 10$ $\varepsilon_{r2} = 2.33$ $\varepsilon_{r3} = 1.0$ $d_1 = d_3 = 0$

VIII. Future Work

Indicating in Section VII (B), we observe that the results of the simulation can be used to represent the sensitivity of the variation of b/d_2 to the performance and the resonant frequency. Base on this observation, it will lead to the future study on the sensitivity of the microstrip structure by applying Cole-Cole performance model.

IX. Conclusion

The proposed model in this research is simple yet practical, and it illustrates the performance of probe-fed rectangular patch antenna for smartphones and portable computer applications. The proposed model can also be used for single layer and multilayer microstrip patch design. Simulation results indicated that the model proposed in this research is compatible with CAD applications. The proposed model is a simple calculation and is valuable contribution as it permits quick and easy design forRF/Microwave engineers.

References

[1] E. Yamashita, K. Atsuki, and T. Veda, “An accurate dispersion formula of microstrip line for computer-aided design of microwave integrated circuit,” *IEEE Trans. Microwave Theory Tech*., vol. MTT-27, pp. 1036-1038, Dec. 1979.

[2] A. K. Verma and R. Kumar, “A new dispersion model for microstrip line,” *IEEE Trans. Microwave Theory Tech*., vol. MTT-46, pp. 1183-1187, Aug. 1998.

[3] I. J. Bahl and S.S. Stuchly, “Analysis of a microstrip covered with a lossy dielectric,” *IEEE Trans. Microwave Theory Tech*., vol. 28, pp. 104-109, 1980.

[4] I. J. Bahl, P. Bhartia, and S. Stuchly, “Design of microstrip antennas covered with a dielectric layer,” *IEEE Trans. Antennas Propagat.*, vol. 30, pp. 314–318, 1982.

[5] M. D. Despande and M.C. Bailey, “Input impedance of microstrip antennas,” *IEEE Trans. Antennas Propagat*, vol. 30, pp. 645- 650, 1982.

[6] A. Bhattacharyya and T. Tralman, “Effects of dielectric superstrate on patch antennas,” *Electron. Lett*., vol. 24, pp. 356–358, 1988.

[7] J. Svaˇcina, “Analysis of multilayer microstrip lines by a conformal mapping method,” *IEEE Trans. Microwave Theory Tech.*, vol. 40, pp. 769–772, 1992.

[8] A. Verma and Z. Rostamy, “Resonant frequency of uncovered and covered rectangular microstrip patch using modified Wolff model,” *IEEE Trans. Microwave Theory Tech*., vol. 41, pp. 109–116, 1993.

[9] R. Shavit, “Dielectric cover effect on rectangular microstrip antenna array,” *IEEE Trans. Antennas Propagat*., vol. 42, pp. 1180–1184, 1994.

[10] S. S. Zhong, G. Liu, and G. Qasim, "Closed form expressions for resonant frequency of rectangular patch antennas with multi dielectric layers," *IEEE Trans. Antennas Propagat*., vol. 42, pp. 1360–1363,1994.
[11] J. T. Bernhard and C. J. Tousignant, "Resonant Frequencies of Rectangular Microstrip Antennas with Flush and Spaced Dielectric Superstrates," *IEEE Trans. Antennas Propagat.*, vol. 47, no. 2, pp. 302 – 308, 1999.
[12] A. K. V. Nasimuddin, "The input impedance of rectangular microstrip patch antenna with iso/anisotropic substratesuperstrate," *IEEE Microwave and wireless component letters*, vol. 11, no. 11, pp. 456-458, 2001.
[13] N. G. Alexopoulos and D. R. Jackson, "Fundamental superstrate (cover) effects on printed circuit antennas," *IEEE Trans. Antennas Propagat*., vol. 32, pp. 807–816, 1984.
[14] M. Biswas and D. Guha, "Input impedance and resonance characteristic of superstrate loaded triangular microstrip patch," *IET Microw. Antennas Propagat*., vol. 3, pp. 92 – 98, 2009.
[15] M. Sen and M. Biswas, "Cad Model to predict the effect of Randome on the Characteristics of Rectangular Patch Antenna," I*nternational Journal of Engineering Science and Technology*, vol. 5, no. 3, March 2013.
[16] H. A. Wheeler, "Transmission-line properties of parallel strips separated by a dielectric sheet," *IEEE Trans. Microwave Theory Tech*., vol. 13, pp. 172–185, 1965.
[17] S. Malisuwan and J. Sivaraks, "Design of Three-Layer Shielded Microstrip Line for Microwave Circuit Applications by Applying Cole-Cole Diagrams," *International Journal of Future Computer and Communications*, vol. 2, no. 5, Oct. 2013.
[18] E. Riande and E. Saiz, *Dipole Moments and birefringence of Polymers*, New Jersey, Prentice Hall, 1992.
[19] F. Abboud, J. P. Damiano, and A. Papiernik, "Simple model for the input impedance of coax-fed rectangular microstrip patch antenna for CAD," *IEE Proc. Microw. Antennas Propag.*, vol. 135, pp. 323- 326.
[20] M. Kirschning, R. H. Jansen, and N. H. L. Koster, "Accurate model for open end effect of microstrip lines," *Electron. Lett.*, vol. 17, pp. 123–125, Feb. 1981.
[21] S. Chattopadhyay, M. Biswas, J. Y. Siddiqui, and D. Guha, "Input impedance of probe-fed rectangular microstrip antennas with variable air gap and varying aspect ratio," *IET Microw. Antennas and Propagat*., vol. 3, pp. 1151-1156, 2009.
[22] S. Malisuwan, P. S. Neelakanta, and V. Ungvichian, "A Cole-Cole diagram representation of microstrip structure," *Journal of the Applied Computational Electromagnetics Society*, vol. 15, no. 3, 2000.
[23] S. Malisuwan, M. Charoenwattanaporn, U. Goenchanart, and V. Ungvichian, "Microstrip Antenna for wireless LAN Applications by applying Modified Smith-Chart Representation," *International Journal of Computer, Internet and Management*, vol. 11, no. 3, 2003.
[24] R. Garg, P. Bhartia, I. Bahl, and A. Ittipiboon, *Microstrip Antenna Design Handbook*, Artech House, 2001.
[25] P. Debye, *Polar Molecules*, Chemical Catalogue Co NY, 1929.
[26] P. S. Neelakanta, *Handbook of Electromagnetic Materials: Monolithic and Composite Versions and Applications. Boca Rato*n, FL: CRC Press, 1995.

Settapong Malisuwan was born on 24th March 1966 in Bangkok, Thailand. He received his PhD in electrical engineering (telecommunications), specializing in mobile communication systems from Florida Atlantic University (State University System of Florida), Boca Raton in 2000. He received an MSc in electrical engineering in mobile communications system, from George Washington University in 1996, an MSc in electrical engineering in telecommunication engineering from Georgia Institute of Technology in 1992 and a BSc in electrical engineering from the Chulachomklao Royal Military Academy, Nakhon-Nayok, Thailand in 1990. He served in the Royal Thai Armed Forces for more than 25 years and is currently the Vice Chairman of National Broadcasting and Telecommunications and the chairman of Telecommunication Commission Bangkok, Thailand. His research interests are in electromagnetics, efficient spectrum management and Telecommunications policy and management.

Wassana Kaewphanuekrungsi was born on 1st February 1979, Bangkok, Thailand. She received her B.S. in Statistics from Chulalongkorn University, Thailand, 2000, and M.S. in Technology Management from Thammasat University, Thailand, 2006. She joined National Broadcasting and Telecommunication Commission (NBTC) as Assistance to Vice Chairman of NBTC in December 2011, which is responsible in the field of telecommunications planning and microstrip antenna design. Previously in 2010, she worked for as senior system analyst at Bangkok Insurance (Public)Co.,Ltd. Her research interests are in information technology, telecommunication technology, wireless communication and antenna design.

Jesada Sivaraks was born on 12th May 1970 in Bangkok, Thailand. He received his MSEE degree from Oklahoma State University in 1996 and BEng from King Mongkut"s Institute of Technology, Thailand. He completed his PhD in electrical engineering at Florida Atlantic University, Boca Raton, FL in 2001. Since 2011, he has been working in National Broadcasting and Telecommunications Commission as the Secretary to the Vice Chairman. His PhD work is on the system aspects of Bluetooth, WLAN and Mobile IP/CDPD. His current research interests are in telecommunication planning and related system analysis and efficient spectrum management. He is a member of Tau Beta Pi, Florida Epsilon and was an Honorary Advisory's Chairman of Science & Technology committee of Parliament in 2009.

Nattakit Suriyakrai was born in Khonkhaen, Thailand on 22nd March, 1987. He received his Bachelor of Liberal Arts in Japanese Language from Thammasat University in 2010. He has been working as an Assistant to Vice Chairman in National Broadcasting and Telecommunications, Bangkok, Thailand since November 2012. His research interests are in technology management and spectrum management.